IGARSS 2023 - 2023 IEEE International Geoscience and Remote Sensing Symposium | 979-8-3503-2010-7/23/$31.00 ©2023 IEEE | DOI: 10.1109/IGARSS52108.2023.10281982

IMPACTS OF FULLY ILLUMINATED TARGETS ON PARTIALLY SHADED BACKGROUNDS FOR A MULTICLASS SUBPIXEL TARGET DETECTION SCENARIO

Chase Cañas[1], *John P. Kerekes*[1], *Colin J. Maloney*[1], *Emmett J. Ientilucci*[1], *Scott D. Brown*[1]

[1]Rochester Institute of Technology, Center for Imaging Science, Rochester, NY 14623

ABSTRACT

Objects on Earth with 3-dimensional geometries cast shadows onto the underlying background due to the obstruction of direct solar radiation. This phenomenon is considered for a multiclass subpixel target detection scenario, where the mixed pixels consist of materials from varying percentages of an illuminated target and partially shaded background. Hyperspectral data collected from UAS-based instruments and novel subpixel targets were used for the analyses. The novel targets enabled empirical observations of fully illuminated targets on partially shaded backgrounds. To assist in developing inferences on the impacts of detection, model reflectance spectra were generated for mixed pixels with fully illuminated and fully shaded background conditions. The modeling approach was validated with the empirical observations. The results imply the shadow effect is an important system parameter for subpixel target percentages of 20% or less, for the multiclass scenario and particular targets explored.

Index Terms— shadow, hyperspectral, novel targets, remote sensing, linear unmixing, object detection

1. INTRODUCTION

Target detection in hyperspectral image processing uses the unique chemical and radiometric properties of materials to differentiate rare targets in the scene relative to (most often) a multiclass background. If the size of the target is smaller than the ground sample distance (GSD) between pixels, the target is subpixel and is mixed with either one or more background materials.

In the spectral community, preexisting research on the impacts of shaded targets have been investigated [1]. However, studies on the impacts of illuminated targets mixed with shaded backgrounds are more scarce. In real scenarios, these situations do occur more frequently than some may consider. Any 3-dimensional object or target of interest, will cast a shadow onto the ground with varying size and intensity depending on the solar angle and optical depth of the Earth's atmosphere. An example scenario is shown in Fig. 1, using a DIRSIG (Digital Imaging and Remote Sensing Image Generation) demo to model the effects.

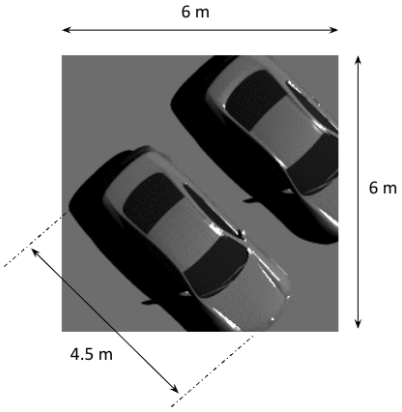

Fig. 1: 3D rendering of an illuminated car casting a shadow on an arbitrary background. Given a GSD of 6m, the subpixel target is illuminated and mixed with a partially shaded background.

1.1. Radiometric Properties of Shaded Materials

The characteristics of a spectral signature (i.e. shape and magnitude) measured from a sensor are dependent on radiometric interactions between the illumination source, atmospheric medium, and material under observation. In remote sensing, the upwelling radiance measured from a visible and near-infrared (VNIR) sensor consists of direct and in-direct (i.e. diffuse) components of solar energy reflected from the target. This also includes solar energy reaching the sensor from surrounding objects in the scene (i.e. adjacency effect) and scattering in the atmosphere (i.e. path radiance).

When an object is shaded, the direct component of solar radiance is obscured. Thus, the upwelling radiance measured by a remote sensor is derived entirely from indirect or diffuse solar interactions. In this case, the spectral signature of the illumination source changes in both shape and magnitude. Therefore, it is improper to assume the spectral signature of a shaded material is simply a scaled version of the illuminated material. In fact, the signatures between a shaded and illuminated material will change in both shape and magnitude.

This work was supported in part by NGA University Research Initiative grant HM04762110005. Approved for public release, NGA-U-2022-02613.

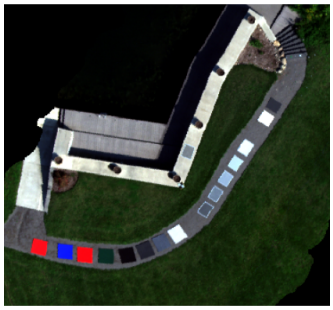

Fig. 2: RGB render of hyperspectral data collected from a 272-band Headwall Nano sensor onboard a DJI Matrice UAV.

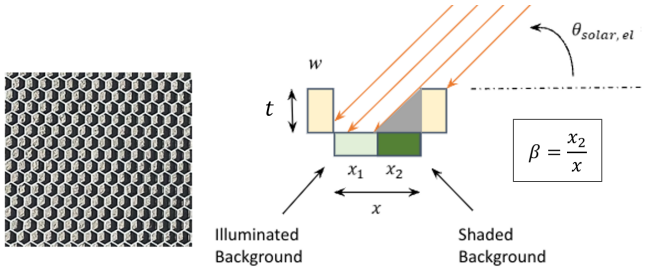

(a) (b)

Fig. 3: (a) 2D model of a novel subpixel target and (b) ray tracing illustration of the novel target impinging a shadow onto the background due to the inherent thickness w.

1.2. Hyperspectral Dataset

A hyperspectral dataset was recently curated using novel targets and UAS-based instruments from the Digital Imaging and Remote Sensing Laboratory (DIRS) at RIT. The data were collected on September 9, 2022 in Rochester, NY at the Tait Preserve, a 177 acre estate recently gifted to RIT in 2019 for expanding interdisciplinary research in the university.

All analyses were performed using atmospherically compensated reflectance data, which was processed using the empirical line method (ELM). Several flight lines of hyperspectral data were collected, however, a sub region where the man-made targets were deployed is shown in Fig. 2. These targets include an assortment of RGB and grayscale felt panels, calibration panels, and novel subpixel targets.

2. METHODOLOGY

2.1. Novel Subpixel Targets

Novel subpixel targets were designed, developed and deployed for the September 9, 2022 data collection. The new design expanded the functionality of earlier versions of the targets [2] to enable the retrieval of hundreds of subpixel target samples with constant subpixel percentages. This was attributed to the large ($\approx$ 3 ft x 4 ft) overall dimensions of the target relative to the small ($\approx$ 4 cm) spatial resolution of the UAS remote sensor. The targets are geometrically flat, with a lattice-like structure fabricated using precision cutting onto $t = 1/4$ inch hardwood. An example 2D model of the design is shown in Fig. 3(a). The inner wall thickness, w, of the lattice directly determines the constant target percentage of subpixel samples collected within the lattice inner region.

For the data collection, five targets ($\approx$ 3 ft x 4 ft) were fabricated with constant nominal target percentages of 20%, 40%, 60%, 80% and 100%. The targets were painted with a gray matte finish (to reduce BRDF effects) and placed on a near-uniform gravel material. The gray perceivable color of the painted target and gravel background was intended to increase spectral similarity, or detection difficulty given the sensor was constrained to the visible and near infrared (VNIR).

The 2-dimensional geometry of the novel target ensures the material in the foreground (i.e. gray painted wood) is fully illuminated. However, the 3-dimensional thickness ($t = 1/4$ inch) of the target also creates a shadow which impinges onto the material in the background (i.e. gravel). This effect occurs repeatedly across the target, given the lattice-like structure. A visualization is shown in Fig. 3(b), where ray tracing is used to demonstrate a shadow being cast between a single cavity of the lattice. The fraction of background material which is partially shaded, $\beta = x_2/x$, depends on the solar elevation angle and the distance, x, between the inner walls of the lattice. The inner wall thickness, w, which changes for each lattice directly changes the inner wall distance, x. Therefore, the percentage of the background that is partially shaded changes across each lattice. A table outlining the percentages of the shaded background for each corresponding nominal target percentage for a given lattice is shown in Table 1. The shaded background percentages were derived using spectral linear unmixing, given there may be slight variations from the nominal values calculated strictly using geometry. This is due to the orientation of the targets may not have been perfectly horizontal relative to the solar angle; any warping in the wood will create deviations from the nominal values.

Table 1: Nominal subpixel target and shaded background percentages characterized across each novel target. The solar zenith angle during time of collect was $\theta_s \approx 51°$.

Subpixel Target α [%]	20	40	60	80	100
Shaded Background β [%]	56	70	81	83	0

The inherent design of the novel targets "self shadowing" effect onto the underlying background demonstrates the phenomenology of a fully illuminated target on a partially shaded background, and motivates the current research under investigation. The unique contribution to the spectral community is the observation of real samples with near-constant fractions of an illuminated target mixed with a partially shaded background. Endmembers of the fully illuminated target (i.e. gray

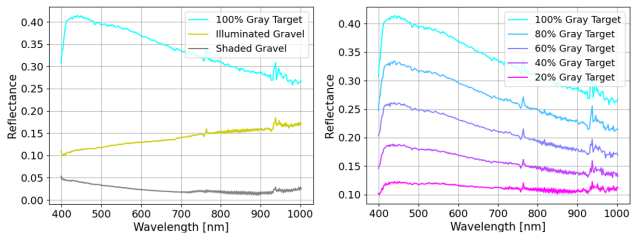

(a) (b)

Fig. 4: (a) Full pixel endmembers of target and background and (b) actual mixed spectra collected across novel targets.

painted wood), fully illuminated background (i.e. gravel), and fully shaded background (i.e. shaded gravel) are shown in Fig. 4(a). The actual mixed spectra across the lattice subpixel targets are shown in Fig. 4(b). These spectra were all derived through averaging hundreds of samples across regions in the hyperspectral dataset.

2.2. Linear Mixture Modeling

Real observations across the lattice targets depict target samples with a partially shaded background, with varying shade fractions β as shown in Table 1. To assess detection impacts at extrema conditions of the shade parameter, synthetic mixed spectra were generated using a linear mixture model. Mixed targets with fully illuminated ($\beta = 0$) and fully shaded ($\beta = 1$) backgrounds were generated using random sampling from empirical distributions of 300-400 samples per subpixel group of 20%, 40%, 60%, 80% and 100%. Thus, the model approach is empirically-driven, so the effects of the atmosphere (e.g. absorption features), sensor (e.g. noise), and material variability are incorporated into the synthetic mixtures. To validate the model approach, synthetic spectra were generated for partially shaded backgrounds with β values derived from the lattice targets. An equivalent numbers of samples between real and synthetic distributions was established.

If a pixel consists of a linear mixture of material from a target and single background class,

$$\mathbf{x}_1 = \alpha \cdot \mathbf{x}_T + (1-\alpha) \cdot \mathbf{x}_B \tag{1}$$

where α is the subpixel target fraction, and $\mathbf{x_T}, \mathbf{x_B}$ are the target and background spectra. This expression represents the cases when the background of a mixed pixel is either fully illuminated or fully shaded. If a pixel consists of a linear mixture of material from a target and two background classes,

$$\mathbf{x}_2 = \alpha \cdot \mathbf{x}_T + \beta(1-\alpha) \cdot \mathbf{x}_{B_1} + (1-\beta)(1-\alpha) \cdot \mathbf{x}_{B_2} \tag{2}$$

where α is the subpixel target fraction, β is the subpixel fraction of background material 1, $(1-\beta)$ is the subpixel fraction of background material 2, and $\mathbf{x_T}$, $\mathbf{x}_{B_1}$, $\mathbf{x}_{B_2}$ are the target and background spectra. This expression represents the case when the background of a mixed pixel is partially shaded (e.g. the lattice targets).

2.3. Target Detection for a Multiclass Background

Real scenarios in subpixel target detection typically consist of a rare target implanted into a diverse scene of multiclass background clutter. Therefore, a similar scene was constructed for the detection analyses, using regions of interest (ROI) across the HSI data shown in Fig. 2. A list of background classes and corresponding proportions of the scene are shown in Table 2.

Table 2: Background classes and corresponding percentages which comprise the scene.

Background Class	Proportions of Scene [%]
Illuminated Gravel	3.37
Shaded Gravel	0.16
Illuminated Concrete	7.01
Shaded Concrete	0.09
Illuminated Wood Deck	9.69
Shaded Wood Deck	9.62
Illuminated Grass	69.30
Light Gray Felt	0.41
White Permaflect	0.33

For the detection analyses, a matched filter algorithm was applied to both the empirical and model spectra,

$$w_{MF}(\mathbf{x}) = \frac{(\mathbf{x}-\boldsymbol{\mu}_B)^T \boldsymbol{\Sigma}^{-1} (\mathbf{t}-\boldsymbol{\mu}_B)}{(\mathbf{t}-\boldsymbol{\mu}_B)^T \boldsymbol{\Sigma}^{-1} (\mathbf{t}-\boldsymbol{\mu}_B)} \tag{3}$$

where $\mathbf{t}$ is the target reference spectrum, $\mu_\mathbf{B}$ is the mean spectrum of the background, $\mathbf{\Sigma^{-1}}$ is the inverse covariance matrix of the background, and $\mathbf{x}$ is a test spectrum. The algorithm was mean-centered using samples across all the background classes listed in Table 2. The target reference spectrum was selected using the average of hundreds of image samples collected across the central region of the 100% full pixel target. After collecting the output scores from the detector algorithm, receiver operating characteristic (ROC) curves were used to evaluate detection across various conditions.

3. RESULTS

3.1. Validation of Synthetic Spectra

The averages of the synthetic and empirical reflectance spectra are shown in Fig. 5. The partially shaded spectra are shown in *green* for the synthetic data and *red* for the real data. The close co-agreement between spectra across each lattice target (20%, 40%, 60%, 80%), validates the efficacy of the linear mixture approach. In addition, the fully illuminated and fully shaded spectra for the synthetic data are shown in *blue* and *orange* in Fig. 5, respectively. These were included as a comparative reference to the partially shaded cases.

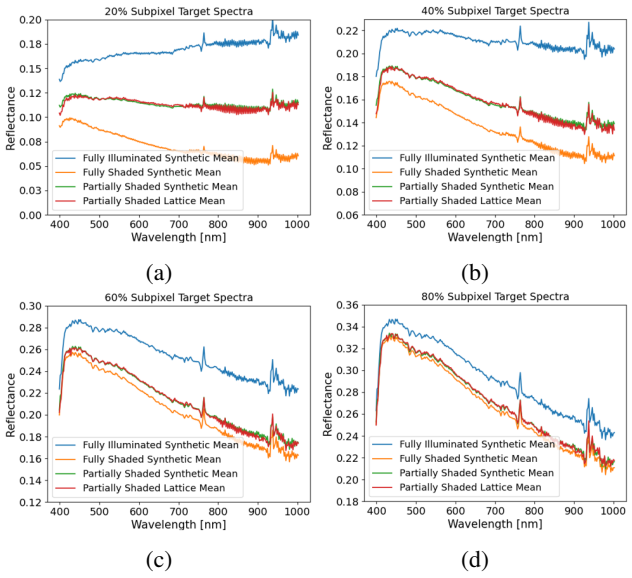

Fig. 5: Comparison of average reflectance spectra between real (red) and synthetic (green, blue, orange) cases for subpixel target percentages (a) 20% (b) 40% (c) 60% & (d) 80%.

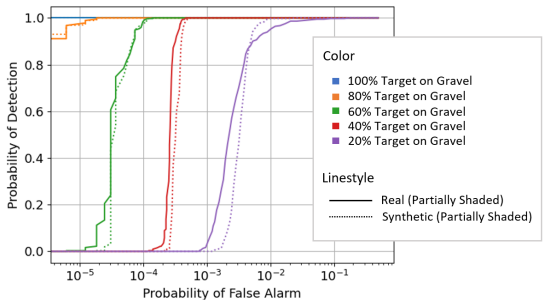

Fig. 6: Comparison of real and synthetic ROC curves for fully illuminated subpixel targets with a partially shaded background.

3.2. Impacts on Detection

The ROC curves derived from the five lattice subpixel targets, in comparison to the synthetic linear mixtures, are shown in Fig. 6. Each curve has a unique shape, driven by multiclass background clutter in the scene. The collection of synthetic ROC curves derived from cases of partially shaded, fully illuminated, and fully shaded backgrounds are shown in Fig. 7.

Considering the multiclass scenario of a fully illuminated target on a partially shaded background, good co-agreement is observed between the empirical and model ROC curves shown in Fig. 6 and Fig. 7, which further validates the model approach. Considering the cases of a fully illuminated and fully shaded background, the model ROC curves in Fig. 7 reveal there are minimal differences for subpixel target percentages of 40% or greater. However, impactful differences are observed for the subpixel target percentage of 20%.

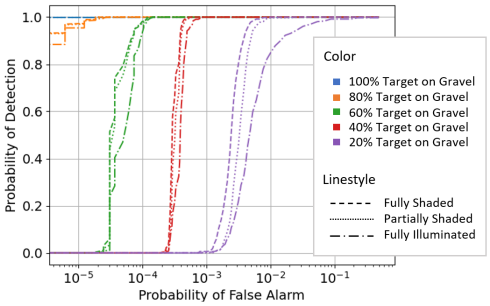

Fig. 7: Synthetic ROC curves for fully illuminated subpixel targets with varying proportions of shaded background.

4. CONCLUSION

In subpixel target detection, the effects of a fully illuminated target impinging a partial shadow within the background of a mixed pixel of a multiclass scenario was considered. Empirical observations of this phenomenon were collected from a hyperspectral dataset curated using novel targets, which provided hundreds of samples of constant target percentages, not found in existing data collections. Synthetic spectra were generated to assess detection impacts for extrema conditions of the shade parameter β (i.e. 0% and 100%), and was validated using the novel targets. The results imply for subpixel target percentages of 20% or less, the shadow effect noticeably impacts detection, as observed in the model ROC curves. Specifically, detection improves when the background is fully shaded, which is sensible given contrast increases between illuminated and shaded materials. It is thus suggested this phenomenon may be an important consideration in the remote sensing system when assessing detection limits. These inferences are not generalized for all scenarios, however, as results were derived for a specific multiclass scene with specific target and background classes. Further research is needed to explore impacts of the shadow effect for smaller subpixels targets less than 20% and other combinations of mixed target and background spectra implanted into other scenes.

5. REFERENCES

[1] E. J. Ientilucci, "SHARE 2012: analysis of illumination differences on targets in hyperspectral imagery," in *Algorithms and Technologies for Multispectral, Hyperspectral, and Ultraspectral Imagery XIX*, vol. 8743. SPIE, May 2013, pp. 125–136.

[2] C. Cañas, J. P. Kerekes, E. J. Ientilucci, and S. D. Brown, "Empirical validation of a hyperspectral systems model for subpixel target detection using data from a new UAS field collection," in *Imaging Spectrometry XXV: Applications, Sensors, and Processing*, vol. 12235. SPIE, Sep. 2022, pp. 98–103.